ASEAN
Journal of Scientific and Technological Reports
Online ISSN:2773-8752

Research article

Facile Assembly of Herbal-Organic and Inorganic Composite for Enhancing Antioxidant and Antibacterial Efficiency

Sonchai Intachai[1, 2], Thapat Jitthiang[3], Jiraporn Chomanee[3], Panita Sumanatrakul[4], and Tanchanok Poonsin[3*]

[1] Innovative Materials Chemistry for Environment Center, Thaksin University, Phatthalung, 93210, Thailand
[2] Faculty of Science and Digital Innovation, Thaksin University, Phatthalung, 93210, Thailand
[3] Faculty of Education, Thaksin University, Songkhla, 90000, Thailand
[4] Faculty of Engineering, Thaksin University, Phatthalung, 93210, Thailand
[*] Correspondence: tanchanok.p@tsu.ac.th

Citation:
Intachai, S.; Jitthiang, T.; Chomanee, J.; Sumanatrakul, P.; Poonsin, T. Facile assembly of herbal-organic and inorganic composite for enhancing antioxidant and antibacterial efficiency. *ASEAN J. Sci. Tech. Report.* **2026**, *29*(2), e260168. https://doi.org/10.55164/ajstr.v29i2.260168.

Article history:
Received: July 7, 2025
Revised: October 13, 2025
Accepted: October 18, 2025
Available online: January 18, 2026

Abstract: This study focused on the fabrication of multifunctional organic–inorganic composites composed of mixed herbal extracts from mangosteen peel (MP), pomelo peel (PP), and cucumber (CP) peel, biomass-derived activated carbon (AC), and zinc oxide@ZnAl-layered double hydroxide (ZnO@ZnAl-LDH) by a mechanochemical solid–solid process. The as-synthesized composites were characterized using XRD, FT-IR, and zeta potential analyses, and their biological activities were evaluated. The MP/PP/CP@AC/LDH composite exhibited superior antioxidant performance, with IC_{50} values of 136.6 μg/mL for DPPH radicals and 195.8 μg/mL for ABTS radicals, which were significantly lower than those of single-extract or single-host systems. The enhanced radical-scavenging behavior was attributed to the synergistic host–guest and guest–guest interactions among ZnO, ZnAl-LDH, AC, and bioactive compounds. Moreover, the composite demonstrated the pronounced antibacterial activity against *Staphylococcus aureus* and partial inhibition toward *Escherichia coli*, owing to reactive oxygen species (ROS) generation and membrane disruption. These findings suggested that MP/PP/CP@AC/LDH was a promising multifunctional herbal material for antioxidant and antimicrobial applications.

Keywords: Herbal extract; Zinc oxide; ZnAl-layered double hydroxide; antioxidant; antibacterial

1. Introduction

In Thailand, herbal remedies have for a long time played a significant role in drug, healthy innovation, and healthcare and body-cleaning goods [1, 2], especially, herbal extracts from mangosteen, pomelo, and cucumber, which are known for their remarkable antibacterial, antioxidant, moisturizing and anti-aging properties [3-6]. However, several active compounds are unstable organic substances that are easily degraded upon exposure to light, oxygen and chemical reactions, thereby reducing biological effectiveness [7]. Typically, the application of herbal extract-based ingredients is preferred in the solid state, because they are easy to use, cost-effective to store, and relatively stable [8]. To address, many attempts have been made to encapsulate crude extracts by surfactant [9] and inorganic host [10]. Furthermore, the antioxidant performance remains steadily high over a long period [7, 9]. In particular, the incorporation of herbal extract in activated carbon (AC) has received much interest as a host-

guest material, as the results of its stable 3D carbonaceous structure, low toxicity, large surface area and H-bonding active sites [11]. Moreover, AC also supports higher stability of organic compounds, and acts as an efficient adsorbent of toxic species [12, 13]. Because most crude extracts show lower antibacterial effectiveness than pure essential oil [14], their antibacterial function must be improved by mixing with another material such as metal oxide and metal hydroxide [7, 15].

Zinc oxide (ZnO), a well-known metal oxide, is recognized as an efficient UV-light absorber and antimicrobial agent [16]. Owing to its relatively low toxicity, ZnO particles have been a promising candidate for use in medical devices and pharmaceutical formulations for controlling *Staphylococcus aureus (S. aureus)* and *Escherichia coli* (*E. coli*) infections [15, 17]. However, bulk ZnO particles obtained by using a co-precipitation method exhibit lower biological activity due to the smaller surface area relative to ZnO nanoparticles [17]. The formation of ZnO nanoparticles in/on an inorganic host has been intensively studied because of the larger surface area, higher stability, and multifunctional merits. Layered double hydroxide (LDH), a general formula of $[M_{1-x}^{2+}M_x^{3+}(OH)_2]^{x+}(A^{n-})_{x/n}\cdot yH_2O$, where M^{2+} = divalent metal cation (Mg^{2+}, Co^{2+}, Zn^{2+}, Ni^{2+}), M^{3+} = trivalent metal cation (Al^{3+}, Fe^{3+}, Cr^{3+}), A^{n-} = interlayer anion (CO_3^{2-}, NO_3^-, Cl^-), has received much attention as a host material due to large surface area, anion exchange and swelling capacities, as well as optical, magnetic, antibacterial and catalytic properties [18]. However, LDH structures can be synthesized in various forms by adjusting the types of M^{2+}, M^{3+}, and A^{n-} species. Among them, ZnAl-LDH has been widely utilized for its antibacterial and pharmacological activities [19]. In addition, the incorporation of ZnO particles onto ZnAl-LDH can further tailor its antibacterial efficiency due to the co-functional effect [7].

The present research was focused on the utilization of AC and ZnAl-LDH solid materials for mixing herbal extracts by a mechanochemical solid-solid reaction [20], which was a simple method for generating a mixed herbal extract-powder based on an organic-inorganic host-guest composite. Many studies have reported that the incorporation of herbal organic compounds can provide synergistic effects on biological properties. However, the formation of such materials in the solid state still faces several challenges, including complicated synthesis procedures and the use of toxic substances [8-11]. In this work, the waste peels of mangosteen (*Garcinia mangostana L.*), pomelo (*Citrus maxima*), and cucumber (*Cucumis sativus L.*) were selected to attain organic extracts because they are abundant throughout Thailand, and contain abundant bioactive substances with strong antioxidant activity. The AC was developed from Krajood (*Lepironia articulata* Retz. Domin) residue, which is a waste-to-wealth route. This study aims to create a valuable material for herbal innovation with both efficient antioxidant and antibacterial activities.

2. Materials and Methods

2.1 Materials

Zinc nitrate hexahydrate ($Zn(NO_3)_2\cdot 6H_2O$) and aluminum nitrate nonahydrate ($Al(NO_3)_3\cdot 9H_2O$) were supported by Loba Chemie PVT. LTD. Gallic acid, 2,2-diphenyl-1-picrylhydrazyl (DPPH), and 2,2′-azino-bis(3-ethylbenzothiazoline-6-sulfonic acid-diammonium salt (ABTS)) were obtained from Sigma Aldrich. Folin-Ciocalteu reagent was obtained from Fisher Scientific. Ammonia (NH_3, 98%) and phosphoric acid (H_3PO_4, 98%) were purchased from Asia Pacific Specialty Chemicals LTD. All chemicals are AR-grade substances that were used directly without any characterization.

2.2 Preparation of AC

The long lines of waste Krajood were cut into small pieces, washed several times with water, collected and dried at 110 °C for 24 h, and finally carbonized at approximately 400 °C for 2 h. The black pieces were spun until achieving fine powder through a 60 mesh-sieve, soaked in distilled water containing excess H_3PO_4 under vigorous shaking for 24 h. The resulting powder was washed several times until achieving the supernatant pH ~ 7, separated with a thin white cloth, and dried at 110 °C for 24 h, finally calcined at 900 °C for 2 h. The activated carbon derived from Krajood residue was obtained, which was abbreviated as AC.

2.3 Preparation of ZnO@ZnAl-LDH

Firstly, the aqueous bimetallic mixture was conducted by mixing the appropriate $Zn(NO_3)_2$ and $Al(NO_3)_3$ amount of molar ratio of 3:1, and the concentrated ammonia was slowly dropped until the pH

reached 9.5 under strong magnetic stirring. The reactor was sealed with aluminium foil, and incubated at 80 °C for 24 h. After that, the precipitate was washed multiple times with DI water until obtaining the supernatant pH ~ 7, then separated with centrifugation, and dried at 80 °C for 24 h. The product powder was abbreviated as ZnO@ZnAl-LDH.

2.4 Preparation of herbal extracts

Each herbal peel (mangosteen, pomelo, or cucumber) was washed, cut into small pieces, and dried at 60 °C until its weight was constant. The extraction was soaked in 95% ethanol solvent at room temperature under vigorous shaking for 3 h, and ultrasonicated at 40 kHz for 30 min. To obtain the crude extract, the solution part was collected by a filter, and the mixed solvent was removed by evaporation and followed by freeze-dry. The crude extract of mangosteen, pomelo, and cucumber peels was abbreviated as MP, PP, and CP, respectively.

2.5 Preparation of organic-inorganic composites

The composites between organic (MP, PP, and/or CP) and inorganic (AC and/or ZnO@ZnAl-LDH) species were prepared by the solid-solid reaction, which comprised herbal extract, AC and ZnO@ZnAl-LDH with the weight ratio of 1:1:1. The reaction between 1 g extract and 1 g AC and/or 1 g ZnO@ZnAl-LDH in the presence of 1 mL acetone was carried out by grinding in the mortar for 30 min. For the mixed-extract batches, the total extract mass was 1.00 g, comprising 0.333 g mangosteen (MP), 0.333 g pomelo (PP), and 0.333 g cucumber (CP) (1:1:1 w/w/w), was then mechanically combined with 1.00 g AC and 1.00 g ZnO@ZnAl-LDH for 30 min, yielding composite powder.

2.6 Analysis of total phenolic content

Total phenolic contents of MP, PP, and CP extracts were analyzed by using the Folin-Ciocalteu colorimetric process. The appropriate amount of 10 mg/mL extract solution and 1.0 mL of 10% (v/v) Folin-Ciocalteu reagent were mixed under vortexing for 5 min, and then 1.6 mL of 7.5% (w/v) Na_2CO_3 solution was added under vortexing for further 30 s, and allowed the reaction in the dark for 30 min at room temperature. The absorbance of the resulting solution was measured at 725 nm to determine the total phenolic content (mg GAE/g extract) by the relationship to the calibration curve of gallic acid.

2.7 Antioxidant activities

For DPPH, 1.0 mg of sample was mixed with 5.0 mL of DPPH solution (10 ppm in ethanol), vortexed for 30 s, kept in the dark for 30 min, and read at 517 nm. For ABTS, the radicals were generated by mixing ABTS (7 mM) with potassium persulfate (2.45 mM) at a 1:1 (v/v) ratio in water and keeping the mixture in the dark for 16 h. Before use, the solution was diluted with ethanol to give an initial absorbance of 0.700 ± 0.020 at 734 nm. Then 1.0 mg of sample was added, and the volume was brought to 5.0 mL with the $ABTS^{\bullet+}$ solution, vortexed for 30 s, kept in the dark for 6 min, and read at 734 nm. Antioxidant activity (%) was calculated as the following equation,

$$\text{Antioxidant efficiency (\%)} = [(A_0 - A_s)/ A_0] \times 100$$

where A_0 is the control absorbance, and A_s is the sample absorbance. The half maximal inhibitory concentration (IC_{50}) of antioxidant (μg/mL) was also determined; all measurements were performed in triplicate and reported as mean ± SD.

2.8 Antibacterial activity

The antibacterial activities against *Staphylococcus aureus* (*S. aureus*) and *Escherichia coli* (*E. coli*) were evaluated using the Plate Count Agar (PCA) assay based on cell viability. Initially, the bacteria were precultured on the nutrient agar (NA) at 37 °C for 24 h, then suspended in 0.85% (w/v) NaCl solution, and adjusted to a turbidity of 10^8 CFU/mL. Subsequently, 5% (v/v) inoculum was introduced into 50 mL of nutrient broth (NB), followed by the addition of antibacterial samples. The inoculated cultures were incubated at 37 °C with shaking at 150 rpm for 24 h, where the bacterial viability was assessed using the spread plate technique on PCA at the serial dilutions ranging from 10^{-5} to 10^{-1} in comparison with the untreated control. The

experimental procedures for the preparation of precursors and their composites, as well as the biological evaluations, are summarized in Scheme 1.

2.9 Characterization

X-ray diffraction (XRD) pattern was recorded in the 2θ range of 5-70 ° by a PANalytical Empyrean powder diffractometer. The FT-IR spectra were analyzed by attenuated total reflection-Fourier transform infrared spectroscopy using a G8044AA-Agilent Technologies. Zeta potential of the product powder that was dispersed in DI water at 25 °C was measured using a Zetasizer (Nano ZS, Malvern, Worcestershire, UK). The absorption spectra of the herbal extract, and DPPH and ABTS radicals were investigated by a Shimadzu UV-1700 Pharmaspec UV-VIS spectrophotometer.

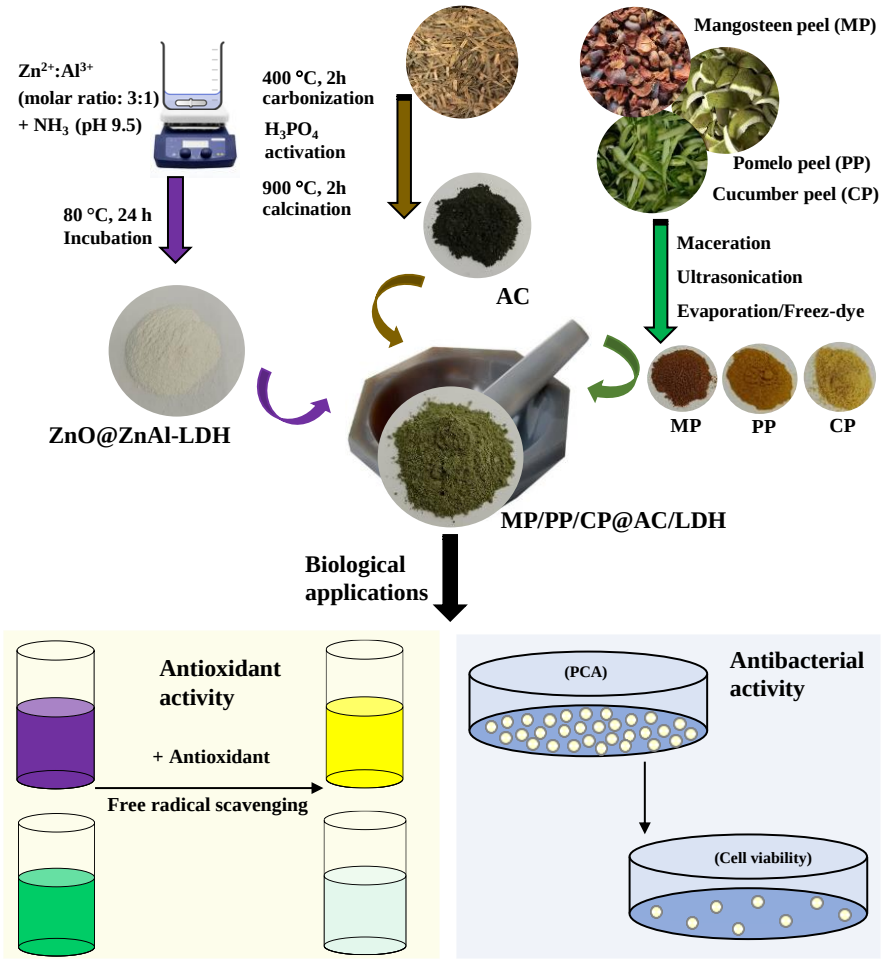

Scheme 1. Representation of preparation of herbal extracts, host materials, organic-inorganic composites, and their biological activities

3. Results and Discussion

3.1 Characterization

The crystalline features of the inorganic hosts and their composites were investigated by the XRD analysis, as depicted in Figure 1. The XRD pattern of AC (Figure 1a) displayed the broad diffraction peaks at 23.9 and 43.6° owing to the (*002*) and (*101*) reflections of a graphitic-like amorphous structure of activated carbon [20]. For ZnAl-LDH (Figure 1b), the diffraction peaks were observed at 11.6, 22.9, 33.8, 38.9, 45.5, 59.9 and 61.4° corresponding to the reflections of (*003*), (*006*), (*012*), (*015*), (*018*), (*110*) and (*113*) of a brucite-like LDH structure, respectively [8,10]. The basal spacing of the (*003*) plane was calculated to be 7.73 Å, and after subtracting the layer thickness (4.8 Å), the interlayer distance was 2.93 Å, which was consistent with the size

of intercalated carbonate ions (CO_3^{2-}) [18]. Additionally, the XRD peaks at 31.8, 34.5, 36.3, 47.5, 56.6, 62.9 and 68.0° were assigned to the (*100*), (*002*), (*101*), (*102*), (*110*), (*103*), and (*112*) planes of ZnO particles, respectively [16,17], indicating the presence of ZnO on the outer surface of ZnAl-LDH. For the MP/PP/CP@AC/LDH composite (Figure 1c), the XRD pattern displayed the reflections corresponding only to ZnAl-LDH and ZnO, with no distinct peaks attributable to AC or the organic extracts due to their low crystallinity [7, 20]. However, the presence of AC and herbal extracts in the composite was further described by later physicochemical characteristics.

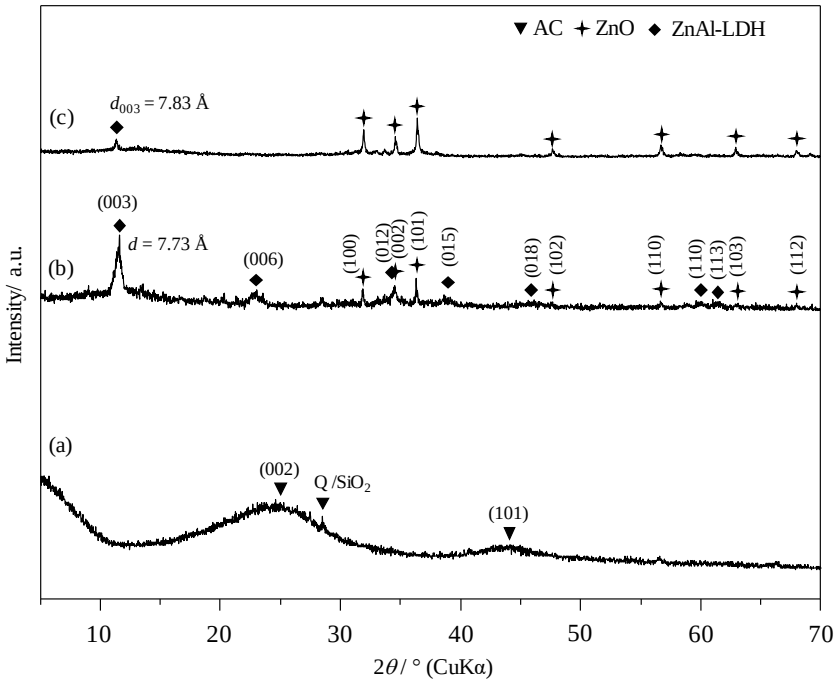

Figure 1. X-ray diffraction patterns of (a) AC, (b) ZnO@ZnAl-LDH, and (c) MP/PP/CP@AC/LDH

To consider the powder colors of the precursors and their corresponding products, ZnO@ZnAl-LDH, AC, and three plant extracts (MP, PP, and CP) showed distinct appearances, as seen in Figure 2. ZnO@ZnAl-LDH appeared white because both Zn^{2+} (d^{10}) and Al^{3+} ions are optically inactive in the visible light region [7]. The black color of AC was attributed to its strong light absorption capacity, resulting in almost no light reflection [20]. Meanwhile, the MP, PP, and CP extracts displayed dark brown, orange-brown, and yellow, respectively, which could be ascribed to the variations in their types and concentrations of bioactive compounds [18]. After the solid-state mixing of these precursors, the resulting composite powder of MP@AC/LDH, PP@AC/LDH, CP@AC/LDH, and MP/PP/CP@AC/LDH exhibited visibly different colors based on greenish-brown (Figure 2f), grayish-green (Figure 2g), yellowish-gray (Figure 2h), and brownish-green (Figure 2i), respectively. The color change might have resulted from blending the physical and chemical merits of white ZnO@ZnAl-LDH, black AC, and yellow-to-brown herbal extracts, suggesting the successful incorporation of AC, ZnO@ZnAl-LDH, and MP, PP, and/or CP in the composites [20].

Figure 2. Physical properties of powders (a) ZnO@ZnAl-LDH, (b) AC, (c) MP, (d) PP, (e) CP, (f) MP@AC/LDH, (g) PP@AC/LDH, (h) CP@AC/LDH, and (i) MP/PP/CP@AC/LDH

The FT-IR spectra were recorded to identify functional groups and confirm interactions among ZnO@ZnAl-LDH, AC, and the representative MP/PP/CP extract mixture. In Figure 3a, the characteristic bands attributed to M–O–M and/or M–O vibration modes appeared below 1000 cm^{-1}, while the broad absorption bands at 3286 and 1636 cm^{-1} were assigned to O–H stretching and H–O–H bending vibration modes of interlayer water, respectively [8, 19]. Additionally, the band at 1359 cm^{-1} corresponded to interlayer carbonate (CO_3^{2-}), confirming the successful formation of the LDH intercalated with CO_3^{2-} [7, 18]. In the FT-IR spectrum of AC (Figure 3b), the weak infrared bands at 1577 and 1027 cm^{-1} were observed, assigning to C=C and C–O vibration modes, in agreement with literature reports for activated carbon [13, 20]. For the MP/PP/CP@AC/LDH composite (Figure 3c), the combination of FT-IR features from ZnO@ZnAl-LDH (3286, 1539, and 1086 cm^{-1}), AC (1577 and 1027 cm^{-1}), and the plant extracts (2853–2962 cm^{-1} for C–H, 1605 and 1442 cm^{-1} for C=C aromatic/alkaloid rings, 1152–1280 cm^{-1} for C–O–C/C–O, and 600–1000 cm^{-1} for C–H out-of-plane) [1-2, 6]. The findings could further confirm that the bioactive organic compounds from the mixed extracts were successfully immobilized onto AC/LDH surface [8, 10].

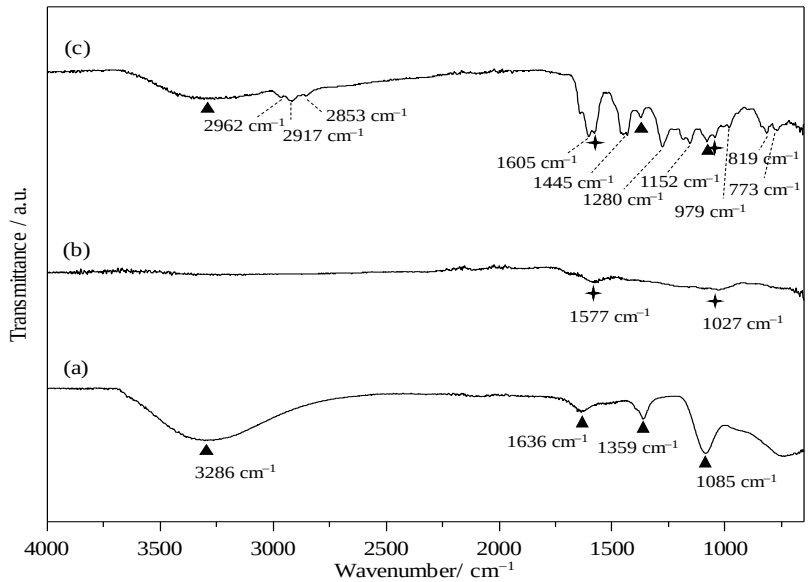

Figure 3. FT-IR spectra (a) ZnO@ZnAl-LDH, (b) AC, and (c) MP/PP/CP@AC/LDH

For further confirmation of the surface charge and interaction, the zeta potential of each sample was measured, as illustrated in Figure 4. It was found that ZnO@ZnAl-LDH, AC, MP, PP, CP, MP@AC/LDH, PP@AC/LDH, CP@AC/LDH and MP/PP/CP@AC/LDH exhibited the zeta potential values of +14.5, –28.2, –4.2, –3.6, –2.9, –11.2, –9.1, –7.7 and –6.8 mV, respectively. By referring, ZnO@ZnAl-LDH displayed positively charged surface because the LDH sheets were generated through the partial substitution of M^{2+} ions with M^{3+} ions [8,10]. In contrast, AC exhibited the negative surface-charge, which was attributed to the presence of functional groups such as hydroxyl (–OH) and carboxyl (–COOH) [20]. Regarding the composites, the zeta potential values were negative and intermediate between those of the pure extracts and AC (namely, more negative than the extracts but less negative than AC). The result might be due to the electrostatic interaction between the negatively charged AC and extracts, and the positively charged ZnO@ZnAl-LDH, confirming the integration of herbal extracts with both AC and ZnO@ZnAl-LDH in the composites [18, 20].

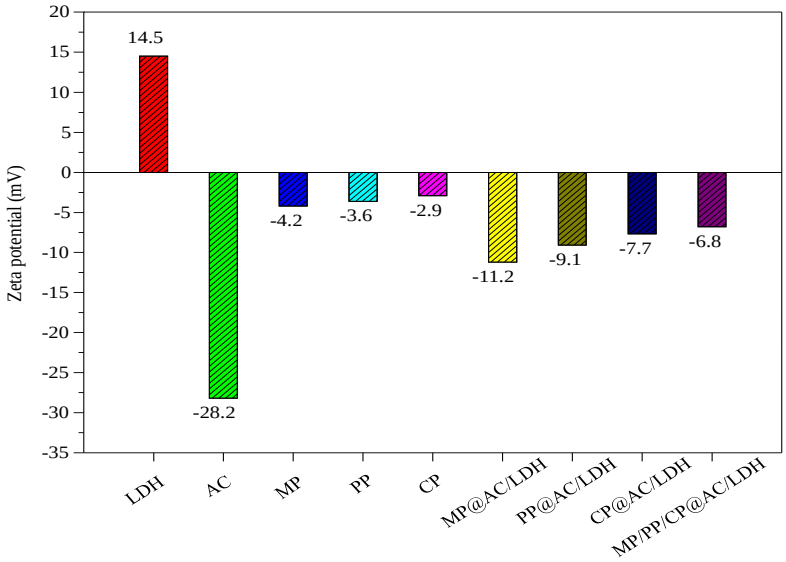

Figure 4. Zeta potential of precursors and composites

Table 1. Total phenolic content and capacity for radical scavenging activities

Material	Total phenolic content (mg GAE/g extract)	DPPH radical scavenging efficiency (%)	ABTS radical scavenging efficiency (%)	IC_{50} of radical scavenging (μg/mL)	
				DPPH	ABTS
ZnO@ZnAl-LDH	-	6.8 ± 0.35	5.6 ± 0.42	-	-
AC	-	1.7 ± 0.35	1.7 ± 0.40	-	-
MP	83.6	97.4 ± 1.79	87.3 ± 0.76	47.5 ± 0.65	61.0 ± 0.44
PP	55.2	86.0 ± 1.62	82.6 ± 0.45	77.3 ± 0.80	102.7 ± 0.72
CP	33.7	67.3 ± 0.71	64.8 ± 0.50	115.5 ± 0.86	143.3 ± 1.21
MP@AC	-	37.4 ± 0.53	33.4 ± 0.45	348.9 ± 1.40	387.7 ± 1.50
PP@AC	-	24.5 ± 0.50	21.1 ± 0.36	433.1 ± 1.21	500.2 ± 1.90
CP@AC	-	15.3 ± 0.50	13.8 ± 0.46	503.7 ± 2.26	563.3 ± 2.15
MP/PP/CP@AC	-	43.7 ± 0.30	40.3 ± 0.55	283.5 ± 1.35	342.5 ± 1.32
MP@LDH	-	48.0 ± 0.67	42.5 ± 0.56	253.1 ± 1.46	297.3 ± 1.23
PP@LDH	-	33.2 ± 0.50	29.1 ± 0.45	383.3 ± 1.53	416.2 ± 1.59
CP@LDH	-	27.6 ± 0.65	23.3 ± 0.56	408.7 ± 1.73	462.3 ± 1.76
MP/PP/CP@LDH	-	52.4 ± 0.62	46.1 ± 0.75	216.4 ± 2.20	247.2 ± 1.80
MP@AC/LDH	-	53.2 ± 0.45	47.8 ± 0.80	196.4 ± 2.10	235.6 ± 1.52
PP@AC/LDH	-	39.2 ± 0.56	33.3 ± 0.60	317.7 ±1.80	354.0 ± 1.31
CP@AC/LDH	-	34.9 ± 0.55	29.5 ± 0.72	366.3 ± 1.88	400.5 ± 1.75
MP/PP/CP@AC/LDH	-	62.4 ± 0.79	57.3 ± 0.35	136.6 ± 0.96	195.8 ± 1.36

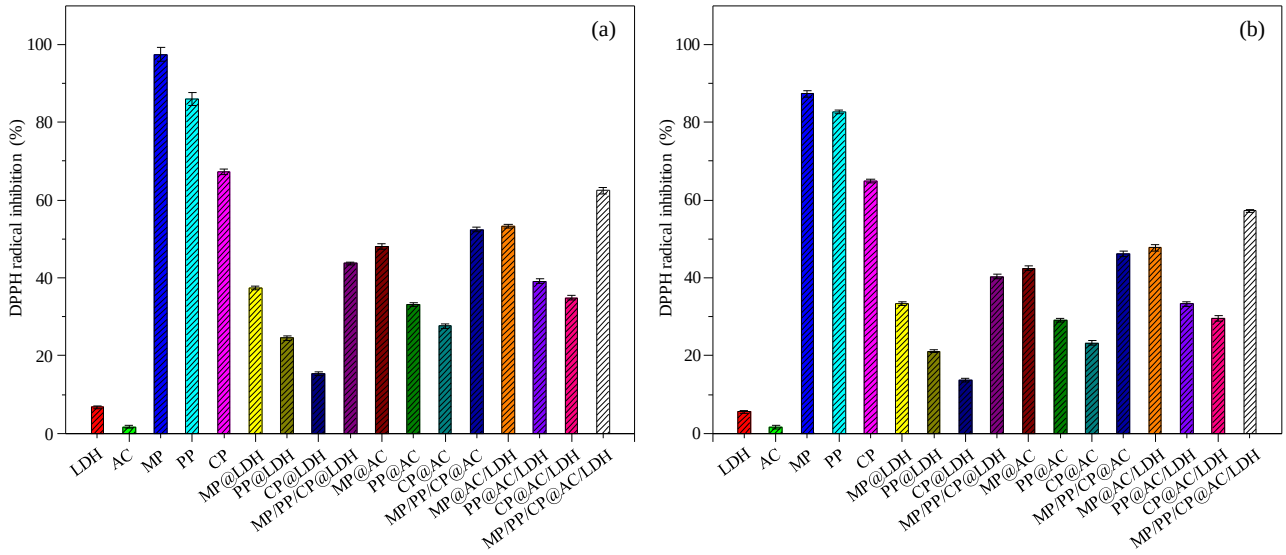

Figure 5. Inhibition efficiency of antioxidants for (a) DPPH radicals and (b) ABTS radicals in the dark.

3.2 Antioxidant activity

The antioxidant activities of various samples, including the herbal extracts (MP, PP, and CP), the host materials (AC, and ZnO@ZnAl-LDH), the composites of extracts with AC (MP@AC, PP@AC, CP@AC, and MP/PP/CP@AC), the composites of extracts with ZnO@ZnAl-LDH (MP@LDH, PP@LDH, CP@LDH, and MP/PP/CP@LDH), and the composites of extracts with both AC and ZnO@ZnAl-LDH (MP@AC/LDH, PP@AC/LDH, CP@AC/LDH, and MP/PP/CP@AC/LDH), were evaluated for scavenging DPPH and ABTS radicals. In Figure 5 and Table 1, the host materials (AC and ZnO@ZnAl-LDH) exhibited very low DPPH and ABTS radical scavenging efficiency (2-7%), suggesting poor antioxidant properties [4, 5]. Whereas all three extracts exhibited relatively high antioxidant activities, indicating strong radical-scavenging potential. In particular, MP showed the highest scavenging efficiencies with 97.4 ± 1.79% for DPPH radicals and 87.3 ± 0.76% for ABTS, compared with PP (86.0 ± 1.62% for DPPH radicals and 82.6 ± 0.45% for ABTS radicals) and CP (67.3 ± 0.71% for DPPH radicals and 64.8 ± 0.50% for ABTS radicals), which could be attributed to its higher total phenolic content (Table 1) [3-6]. For the composites formed between the extracts and ZnO@ZnAl-LDH, the DPPH radical scavenging profile ranged from 28 to 48% for DPPH radicals and 23 to 43% for ABTS radicals, which were higher than those observed in the composites formed with AC alone (15 to 37% for DPPH radicals and 14 to 33 for ABTS radicals). It could be explained by the advantageous properties of ZnO@ZnAl-LDH in the presence of hydroxyl groups and ZnO particles, acting as the effective reducing agents relative to AC [8,10]. Remarkably, by mixing the three extracts with a single host material, the antioxidant efficiencies significantly improved relative to the composites containing only a single extract. The findings might be due to the synergistic effects based on the host-guest and guest-guest interactions [21]. Furthermore, for the extracts combined with both host materials (AC and ZnO@ZnAl-LDH), the as-prepared composites displayed the higher antioxidant efficiency (44-52% for DPPH radicals and 40-46% for ABTS radicals) compared to those containing only a single host. It could be attributed to the cooperative interactions among host-guest and host-guest-host interactions, along with a more uniform distribution of the extracts on the surface of host materials [22, 23]. Importantly, the composite comprising the three extracts and both host materials (MP/PP/CP@AC/LDH) exhibited the highest scavenging inhibition of 62% for DPPH radicals and 57% for ABTS radicals, which might result from the stronger host-guest and host-guest-host interactions [21, 22].

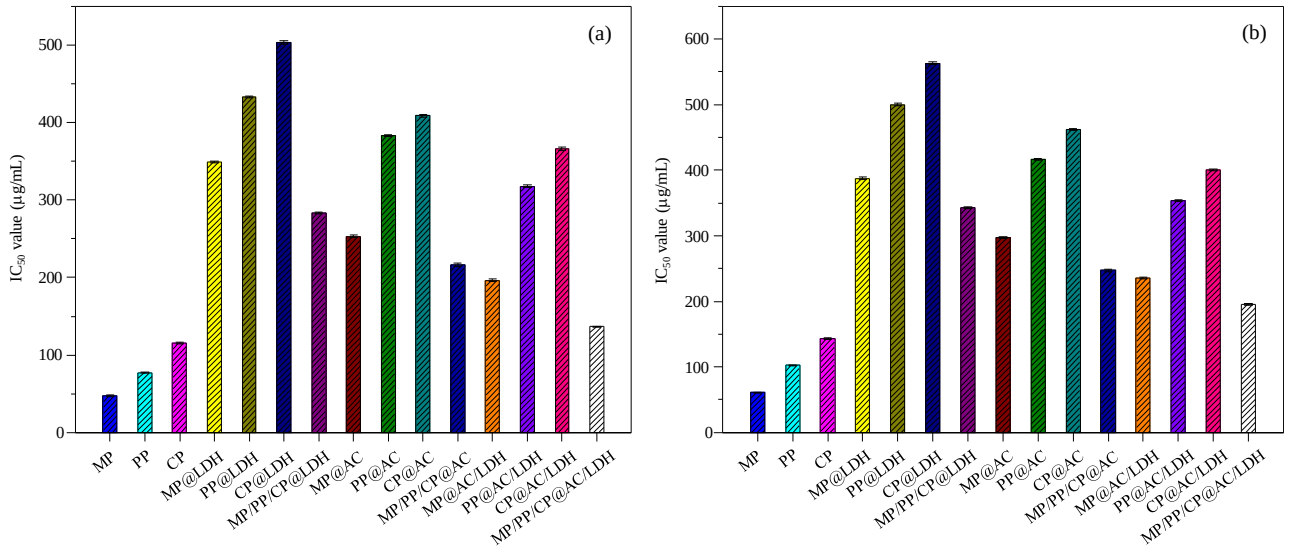

Figure 6. IC_{50} values (concentrations required to achieve 50% inhibition efficiency) of the antioxidant samples for (a) DPPH and (b) ABTS radicals.

The half inhibitory concentrations (IC_{50}) of DPPH and ABTS radicals for MP, PP, CP, MP@AC, PP@AC, CP@AC, MP/PP/CP@AC, MP@LDH, PP@LDH, CP@LDH, MP/PP/CP@LDH, MP@AC/LDH, PP@AC/LDH, CP@AC/LDH, and MP/PP/CP@AC/LDH are depicted in Figure 6 and listed in Table 1. The values ranged from 48–504 and 61–563 µg/mL for DPPH and ABTS radical scavenging activities, respectively, depending on the type of herbal extract, host material, and composite, as described above [1-2, 21-23]. Notably, DPPH showed higher inhibition than ABTS because DPPH was more sensitive to hydrogen-donating antioxidants, while ABTS involved both electron and hydrogen transfer, resulting in lower efficiency [24]. These findings could be indicative that MP/PP/CP@AC/LDH exhibited superior antioxidant performance compared to other herbal extracts such as *Zingiber officinale* extract (201.8 µg/mL) and its composite to LDH (349.2 µg/mL) [25], and essential oil of *Zingiber cassumunar* (1059.9 µg/mL) [26] for inhibiting DPPH radicals. Besides, the as-prepared composite exhibited the higher efficiency compared to Thai traditional herbal formulation, Ya-A (1600 µg/mL) [27], and the isolate of SWUF16-4.1 (283 µg/mL) [28].

Table 2. Antibacterial efficacy of precursors and composites

Antibacterial agents	Number of *S. aureus* viable cells (CFU/mL)			Number of *E. coli* viable cells (CFU/mL)		
	10^{-1}	10^{-3}	10^{-5}	10^{-1}	10^{-3}	10^{-5}
MP PP CP AC	> 300 colony			> 300 colony		
ZnO@ZnAl-LDH	< 30 colony	not detected	not detected			
MP/PP/CP@AC/LDH	not detected	not detected	not detected	> 300 colony	< 30 colony	< 30 colony

3.3 Antibacterial activity

The antibacterial activity against *Staphylococcus aureus* (*S. aureus*) and *Escherichia coli* (*E. coli*) of the herbal extracts (MP, PP and CP), host materials (AC and ZnO@ZnAl-LDH), and the composite (MP/PP/CP@AC/LDH) was evaluated using the plate count agar (PCA) method to determine the number of surviving bacterial colonies, as shown in Table 2. The results revealed that ZnO@ZnAl-LDH inhibited the growth of *S. aureus* more effectively than the single extract (MP, PP, and CP) or the AC host material. Among all tested samples, only ZnO@ZnAl-LDH precursor exhibited excellent antibacterial performance [15]. The antibacterial mechanism of ZnO and/or ZnAl-LDH could be attributed to their ability to generate reactive oxygen species (ROS), such as superoxide and hydroxyl radicals to damage bacterial cell membranes through lipid peroxidation.

Consequently, the loss of some essential substances (sugars, DNA, and proteins) caused the reduction of the bacteria's ability to survive, leading to their death [19]. Interestingly, MP/PP/CP@AC/LDH exhibited the highest antibacterial performance among all samples, which might be the result of the synergistic effect involving multiple integrating-parts of ZnO, ZnAl-LDH, extracts and AC. These phenomena were bases on the host–guest (between the host materials and extracts), guest-guest (among the different extracts), and host-guest-guest interactions, which collectively enhanced the antibacterial efficiency [22, 23]. Most samples exhibited no inhibitory effect against *E. coli*, showing dense bacterial growth (> 300 colonies). Only MP/PP/CP@AC/LDH showed partial inhibition, reducing viable cells to fewer than 30 colonies at higher concentrations. This limited efficacy was observed because *E. coli* possessed a more complex outer membrane structure relative to *S. aureus*, reducing the material's antibacterial penetration [3-5]. Therefore, the incorporation of ZnO@ZnAl-LDH with the mixed plant extracts in the composite significantly improved the antibacterial efficacy against *S. aureus*.

4. Conclusions

Organic–inorganic composite materials were successfully prepared by incorporating mangosteen peel (MP), pomelo peel (PP), and cucumber peel (CP) extracts with activated carbon (AC) and ZnO@ZnAl-LDH as host materials through a simple solid–solid method. The resulting MP/PP/CP@AC/LDH composite exhibited the most efficient antioxidant performance with IC_{50} values of 136.6 μg/mL for DPPH and 195.8 μg/mL for ABTS radicals, which were markedly lower than those of single-extract composites (253–563 μg/mL) or mixed-extract systems containing a single host (216–342 μg/mL). This improvement was mainly attributed to the synergistic effects among host–guest, guest–guest, and host–guest–guest interactions that enhanced the electron- and hydrogen-transfer capabilities of the composite. In terms of antibacterial behavior, ZnO@ZnAl-LDH and MP/PP/CP@AC/LDH effectively inhibited the growth of *Staphylococcus aureus*. In contrast, most samples showed no inhibition toward *Escherichia coli*, only MP/PP/CP@AC/LDH displayed partial *Escherichia coli* suppression, suggesting limited penetration through the Gram-negative bacterial membrane. The incorporation of ZnO@ZnAl-LDH and multiple herbal extracts significantly enhanced both antioxidant and antibacterial properties. These findings highlighted the potential of MP/PP/CP@AC/LDH composite as a multifunctional herbal powder, possessing strong DPPH and ABTS radical scavenging capacity together with antibacterial activity, particularly against *Staphylococcus aureus*, making it a promising candidate for further development in herbal-based cosmetic, pharmaceutical, and hygienic applications.

5. Acknowledgements

The scientific instrument support was gratefully provided by Faculty of Science and Digital Innovation and Faculty of Education, Thaksin University.

Author Contributions: Conceptualization; funding acquisition, T.P.; methodology; investigation, S.I., T.J., and T.P.; writing-original draft preparation, S.I., J.C., P.S and T.P.; writing-review and editing, S.I. and T.P.

Funding: This work was financially supported by the Thaksin University Research Fund, Thailand.

Conflicts of Interest: Declare conflicts of interest or state "The authors declare no conflict of interest."

References

[1] Siriyong, T.; Chanphool, H.; Jitjum, S.; Laohaprapanon, S.; Voravuthikunchai, S. P. Therapeutic Efficacy and Safety of Traditional Thai Herbal Medicines for Insomnia: A Double-Blind Randomized Controlled Trial. *Adv. Integr. Med.* **2025**, *12*, 100459. https://doi.org/10.1016/j.aimed.2025.01.006

[2] Limsuwan, S.; Thammathirata, T.; Yupanquic, C. T.; Wunnoo, S.; Eawsakul, K.; Noonong, K.; Punsawad, C.; Siripithaya, Y.; Bunluepuech, K. In Vitro Antimicrobial and NO Inhibitory Activities of a Thai Herbal Recipe against *Cutibacterium acnes*, *Staphylococcus aureus*, and *Staphylococcus epidermidis*. *Trends Sci.* **2025**, *22*, 9989. https://doi.org/10.48048/tis.2025.9989

[3] Semangoen, T.; Chotigawin, R.; Sangnim, T.; Chailerd, N.; Yodkeeree, S.; Pahasup-anan, T.; Huanbutta, K. Antimicrobial Efficacy of Mangosteen (*Garcinia mangostana*) Peel Extracts in Airborne Microbial

Control within Livestock Farming Environments. *Microb. Pathog.* **2025**, *204*, 107618. https://doi.org/10.1016/j.micpath.2025.107618

[4] Govindaiah, P. M.; Ruban, S. W.; Kiran, M.; Mohan, H. V.; Prabha, R. Exploring the In Vitro Antioxidant and Antimicrobial Properties of Pomelo Fruit Extract in Goat Meat: A Promising Alternative for Preservative and Health Benefits. *Sci. Hortic.* **2024**, *337*, 113534. https://doi.org/10.1016/j.scienta.2024.113534

[5] Anjani; Srivastava, N.; Mathur, J. Isolation, Purification, and Characterization of Quercetin from *Cucumis sativus* Peels: Antimicrobial, Antioxidant, and Cytotoxicity Evaluations. *3 Biotech* **2023**, *13*, 46. https://doi.org/10.1007/s13205-023-03464-8

[6] Xiao, L.; Ye, F.; Zhou, Y.; Zhao, G. Utilization of Pomelo Peels to Manufacture Value-Added Products: A Review. *Food Chem.* **2021**, *351*, 129247. https://doi.org/10.1016/j.foodchem.2021.129247

[7] Intachai, S.; Bosoy, S.; Thepthong, P.; Sumanatrakul, P.; Chanasit, W.; Khaorapapong, N. Effect of ZnAl-LDH-Based Host Material on Optical, Antioxidant, and Antibacterial Characteristics of *Zingiber montanum*. *Chem. Pap.* **2024**, *78*, 4119–4128. https://doi.org/10.1007/s11696-024-03305-9

[8] Kumari, S.; Sharma, V.; Soni, S.; Sharma, A.; Thakur, A.; Kumar, S.; Dhama, K.; Sharma, A. K.; Bhatia, S. K. Layered Double Hydroxides and Their Tailored Hybrids/Composites: Progressive Trends for Delivery of Natural/Synthetic Drug/Cosmetic Biomolecules. *Environ. Res.* **2023**, *238*, 117171. https://doi.org/10.1016/j.envres.2023.117171

[9] Thepthong, P.; Srirat, S.; Hiranrat, W.; Kongsune, P.; Chana, N. Development of Chitosan-Based Microencapsulation System for *Mitragyna speciosa* Alkaloids: A Novel Approach for Alzheimer's Disease Treatment. *J. Pharm. Innov.* **2025**, *20*, 58. https://doi.org/10.1007/s12247-025-09977-4

[10] Bahman, H.; Gharanjig, K.; Ghasemi, E.; Kazemian, H.; Hosseinnezhad, M.; Gharanjig, H. Synthesis and Characterization of an Eco-Friendly Nano-Hybrid Based on Luteolin-Loaded Zinc–Aluminum Layered Double Hydroxide for Biological Applications. *Int. J. Environ. Sci. Technol.* **2025**, *22*, 3545–3566. https://doi.org/10.1007/s13762-024-05960-7

[11] Suárez-Quiroz, M. L.; Campos, A. A.; Alfaro, G. V.; González-Ríos, O.; Villeneuve, P.; Figueroa-Espinoza, M. C. Isolation of Green Coffee Chlorogenic Acids Using Activated Carbon. *J. Food Compos. Anal.* **2014**, *33*, 55–58. https://doi.org/10.1016/j.jfca.2013.10.005

[12] Christodoulou, P.; Ladika, G.; Tsiantas, K.; Kritsi, E.; Tsiaka, T.; Cavouras, D.; Zoumpoulakis, P.; Sinanoglou, V. J. Quality Assessment of Greenhouse-Cultivated Cucumbers (*Cucumis sativus*) during Storage Using Instrumental and Image Analyses. *Appl. Sci.* **2024**, *14*, 8676. https://doi.org/10.3390/app14198676

[13] Zhang, Y.; Fu, X.; Wang, L.; Guo, X.; Dong, B. Sorption of Phenols and Flavonoids on Activated Charcoal Improves Protein Metabolism, Antioxidant Status, Immunity, and Intestinal Morphology in Broilers. *Front. Vet. Sci.* **2024**, *10*, 1327455. https://doi.org/10.3389/fvets.2023.1327455

[14] Zhao, Y.; Wei, J.; Li, C.; Ahmed, A. F.; Liu, Z.; Ma, C. A Comprehensive Review on Mechanism of Natural Products against *Staphylococcus aureus*. *J. Future Foods* **2022**, *2*, 25–33. https://doi.org/10.1016/j.jfutfo.2022.03.014

[15] Bizuayehu, T.; Kassaw, B.; Kendie, M. Green Synthesis, Characterization, and Antibacterial Activity Investigation of Zinc Oxide Nanoparticles Using *Rumex nervosus* Vahl Leaf Extract. *Results Chem.* **2025**, *13*, 102046. https://doi.org/10.1016/j.rechem.2025.102046

[16] Sobhy, M.; Ali, S. S.; Khalil, M. A.; Chen, X.; Cui, H.; Lin, L.; El-Sapagh, S. Exploring the Potential of Zinc Oxide Nanoparticles against Pathogenic Multidrug-Resistant *Staphylococcus aureus* from Ready-to-Eat Meat and Its Proposed Mechanism. *Food Control* **2024**, *156*, 110117. https://doi.org/10.1016/j.foodcont.2023.110117

[17] Almoneef, M. M.; Awad, M. A.; Aldosari, H. H.; Hendi, A. A.; Aldehish, H. A.; Merghani, N. M.; Alshammari, S. G. Exploring the Multi-Faceted Potential: Synthesized ZnO Nanostructure—Characterization, Photocatalysis, and Crucial Biomedical Applications. *Heliyon* **2024**, *10*, e32714. https://doi.org/10.1016/j.heliyon.2024.e32714

[18] Intachai, S.; Sumanatrakul, P.; Khaorapapong, N. Control of Particle Growth and Enhancement of Photoluminescence, Adsorption Efficiency, and Photocatalytic Activity for Zinc Sulfide and Cadmium

Sulfide Using CoAl-Layered Double Hydroxide System. *Environ. Sci. Pollut. Res.* **2023**, *30*, 63215–63229. https://doi.org/10.1007/s11356-023-26461-z

[19] Cardinale, A. M.; Alberti, S.; Reverberi, A. P.; Catauro, M.; Ghibaudo, N.; Fortunato, M. Antibacterial and Photocatalytic Activities of LDH-Based Sorbents of Different Compositions. *Microorganisms* **2023**, *11*, 1045. https://doi.org/10.3390/microorganisms11041045

[20] Intachai, S.; Sumanatrakul, P.; Pankam, P.; Suppaso, C.; Khaorapapong, N. Efficient Removal of Both Anionic and Cationic Dyes by Activated Carbon/NiFe-Layered Double Oxide. *J. Inorg. Organomet. Polym. Mater.* **2022**, *32*, 1999–2008. https://doi.org/10.1007/s10904-022-02254-8

[21] Ma, X.; Zhao, Y. Biomedical Applications of Supramolecular Systems Based on Host–Guest Interactions. *Chem. Rev.* **2015**, *115*, 7794–7839. https://doi.org/10.1021/cr500392w

[22] Acar, T.; Arayici, P. P.; Ucar, B.; Coksu, I.; Tasdurmazli, S.; Ozbek, T.; Acar, S. Host–Guest Interactions of Caffeic Acid Phenethyl Ester with β-Cyclodextrins: Preparation, Characterization, and In Vitro Antioxidant and Antibacterial Activity. *ACS Omega* **2024**, *9*, 3625–3634. https://doi.org/10.1021/acsomega.3c07643

[23] Swarnkar, N.; Kamalakaran, A. S.; Chintha, J.; Kambhampati, N. S. V.; Sripada, L.; Balakrishnan, S. B. Host–Guest Inclusion Complexes of Tafamidis with β-Cyclodextrin: Preparation, Characterization, and In Vitro Antibacterial and Antioxidant Approach. *J. Mol. Struct.* **2025**, *1332*, 141649. https://doi.org/10.1016/j.molstruc.2025.141649

[24] Lang, Y.; Gao, N.; Zang, Z.; Meng, X.; Lin, Y.; Yang, S.; Yang, Y.; Jin, Z.; Li, B. Classification and Antioxidant Assays of Polyphenols: A Review. *J. Future Foods* **2024**, *4*, 193–204. https://doi.org/10.1016/j.jfutfo.2023.07.002

[25] Jeung, D.-G.; Kim, H.-J.; Oh, J.-M. Incorporation of *Glycine max* Merrill Extract into Layered Double Hydroxide through Ion Exchange and Reconstruction. *Nanomaterials* **2019**, *9*, 1262. https://doi.org/10.3390/nano9091262

[26] Leelapornpisid, P.; Chansakaow, S.; Chaiyasut, C.; Wongwattananukul, N. Antioxidant Activity of Some Volatile Oils and Absolutes from Thai Aromatic Plants. *Acta Hortic.* **2008**, *786*, 61–65. https://doi.org/10.17660/ActaHortic.2008.786.5

[27] Mahadlek, J.; Tuntarawongsa, S.; Phaechamud, T. Antioxidant Activity and Total Phenolic Contents of Some Thai Traditional Formulations. *Isan J. Pharm. Sci.* **2017**, *13*, 97–105.

[28] Wangsawat, N.; Nahar, L.; Sarker, S. D.; Phosri, C.; Evans, A. R.; Whalley, A. J. S.; Choowongkomon, K.; Suwannasai, N. Antioxidant Activity and Cytotoxicity against Cancer Cell Lines of Extracts from Novel *Xylaria* Species Associated with Termite Nests and LC–MS Analysis. *Antioxidants* **2021**, *10*, 1557. https://doi.org/10.3390/antiox10101557